2011 50th IEEE Conference on Decision and Control and
European Control Conference (CDC-ECC)
Orlando, FL, USA, December 12-15, 2011

# Fault Diagnosis for Nonlinear Hydraulic-Mechanical Drilling Pipe Handling System

Martin Choux and Mogens Blanke

*Abstract*— **Leakage and increased friction are common faults in hydraulic cylinders that can have serious consequences if they are not detected at early stage. In this paper, the design of a fault detector for a nonlinear hydraulic mechanical system is presented. By considering the system in steady state, two residual signals are generated and analysed with a composite hypothesis test which accommodates for unknown parameters. The resulting detector is able to detect abrupt changes in leakage or friction given the noisy pressure and position measurements. Test rig measurements validate the properties of residuals and high fidelity simulation and experimental results demonstrate the performance and feasibility of the proposed method.**

## I. INTRODUCTION

Hydraulic pistons are indispensable in industrial fields that require high actuation forces. The high difference of pressure needed inside the cylinder chambers in order to deliver the necessary force can be realised only if the leakage between the two chambers is kept small, involving considerable friction against the piston displacement. These two parameters, friction and leakage, play an important role in the reliability of hydraulic systems and their changes are a direct consequence of components' wear. To reduce the cost of maintenance and to prevent such systems from failures, a fault detection for leakage and friction must be considered. However, due to significant nonlinearities in hydraulic systems and the large uncertainties in their parameters, fault detection is difficult to implement in practice.

Numerous techniques have been developed in order to generate residuals for nonlinear hydraulic systems, using artificial neural network in [1], extended Kalman filtering in [2] and robust observers in [3]. Once the residual signal is generated, the fault detector must analyse and process the signal to decide on the presence of a fault. This paper focusses on the design of residual generators for an hydraulic actuator system using statistical change detection algorithms [4], [5], [6]. Diagnosis and fault-tolerant control of a similar system was demonstrated in [7] where a differential geometric approach for fault diagnosis was succesfully demonstrated but the statistical properties of diagnosis were not pursued.

A model was developed in [8] that is representative for a typical nonlinear hydraulic-mechanical system (NHMS) used in a commercial off-shore drilling equipment. The system is used for drilling pipe handling and for operations such as making up a string of drilling pipe. Leakage or increased friction in an actuator could lead to pipe damage or to hazards in operation, so both are essential to diagnose. Residual generation is investigated for this highly nonlinear and parameter-uncertain system, and residuals are determined from which the two high severity faults could be diagnosed. Statistical change detection methods are employed for hypothesis testing about faults and results are validated against a high fidelity simulation model and against experiments.

## II. MODEL DESCRIPTION

The nonlinear hydraulic-mechanical system (NHMS) in [8] was further decomposed, in [9], in a linear hydraulic actuator connected to a mechanical mass-spring-damper system, which could be analysed separately to reduce the complexity of the initial system.

The reduced NHMS is hence considered in this paper with two modifications arising from experience: control valve dynamics can be neglected and system input is then valve opening $u = x_v$; the friction model need be extended to better describe static and dynamic friction phenomena.

Fig. 1 shows a drawing of the system. Pressure sensors provide measurement of pressure difference between the two cylinder chambers $p_L$, also referred to as the load pressure, and displacement sensors measure the position $y$ of the mass element. Total load mass is $M$, equivalent spring coefficient is $k$ and damping is $d$. These parameters are time varying and very uncertain. Before the tool engages with a drilling tube, spring coefficient and damping are literally nil. At engagement, load mass and the $k$ and $d$ parameters jump to high values, and during operation of the tool, plasticity can decrease $k$.

In the real offshore application of the system, too high forces from the cylinder would damage the drilling pipe and too low forces could cause loss of grip of the pipe. High cylinder friction could cause lower forces than needed, but if interpreted by a pressure feedback loop as if the necessary engagement force had been obtained, loss of grip would be at risk. Undetected leakage (change in the leakage coefficient $c_L$) could also cause loss of grip. Therefore, hazardous conditions and associated risks are pertinent for this crucial hydraulic gripping element in an offshore drilling operation,

M. Choux is PhD graduate in the Mechatronics Group, Department of Engineering, University of Agder, N-4892 Grimstad, Norway martin.choux@uia.no

M. Blanke is professor at the Automation and Control Group, Department of Electrical Engineering, Technical University of Denmark, DK-2800 Kgs. Lyngby, Denmark and adjunct professor at CeSOS, Norwegian University of Science and Technology, NO-7491 Trondheim, Norway. mb@elektro.dtu.dk

978-1-61284-799-3/11/$26.00 ©2011 IEEE

unless friction and leakage faults can be reliably diagnosed, and better: reliably prognosed.

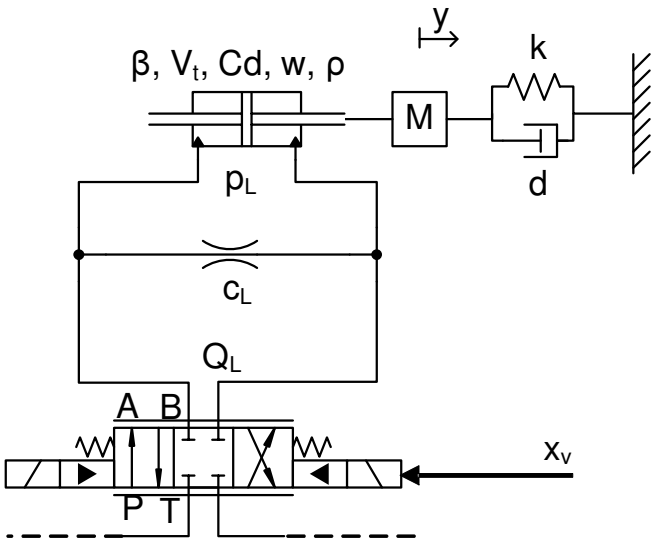


Fig. 1. Nonlinear hydraulic-mechanical system with control valve and hydraulic cylinder exerting forces on the object to be handled. Total load mass $M$, equivalent spring coefficient $k$ and damping $d$ are time varying and very uncertain.

The following equations in hydraulic units (for example $p_L$ in *bar* instead of *Pa*) govern the NHMS:

$$c_1: \quad Q_L = 6000\sqrt{10}\, C_d\, w\, x_v \sqrt{\frac{1}{\rho}(p - \text{sign}(x_v) p_L)} \tag{1}$$

$$c_2: \quad \ddot{y} = \frac{1}{M}\left(\frac{A\, p_L}{10} - k y - d\dot{y} - F_{fric}(z, \dot{y})\right) \tag{2}$$

$$c_3: \quad \dot{p_L} = \frac{4\beta}{V_t}\left(Q_L \frac{50}{3} - A\dot{y} - c_L p_L\right) \tag{3}$$

$$m_1: \quad y_1 = y + w_{1n} \tag{4}$$

$$m_2: \quad y_2 = p_L + w_{2n} \tag{5}$$

$$a_1: \quad u_1 = x_v \tag{6}$$

$$a_2: \quad u_2 = p \tag{7}$$

$$d_1: \quad \dot{y} = \frac{dy}{dt} \tag{8}$$

$$d_2: \quad \ddot{y} = \frac{\dot{y}}{dt} \tag{9}$$

$$d_3: \quad \dot{p_L} = \frac{dp_L}{dt} \tag{10}$$

Eq.(1) represents flow, $Q_L$, through the valve orifice, where $p$ is the supply pressure, $\rho$ is the hydraulic fluid density, $C_d$ is the orifice discharge and $w$ is the opening width. Eq.(2) is acceleration of the actuator tool and the load mass, where $A$ is the cylinder effective area. Eq.(3) is pressure dynamics, where $\beta$ is the hydraulic fluid bulk modulus and $V_t$ is the effective cylinder volume. Eqs.(4) and (5) are position and load pressure measurements where $w_{1n}$ and $w_{2n}$ are measurement noise generated by the electronic devices, considered as thermal noise and modelled as an additive white gaussian noise (WGN) with zero mean.

Friction inside the cylinder has significant effects in the performances of position tracking and change in one of its parameter could have severe consequences. In order for the friction model to accurately represent static phenomena such as Coulomb friction and the Stribeck effect, as well as dynamic friction phenomena, including pre-sliding displacement and hysteresis, a LuGre model [10] was chosen, which is described by the following equations:

$$c_4: \quad F_{fric} = \sigma_0 z + \sigma_1 \dot{z} + \sigma_2 \dot{y} \tag{11}$$

$$c_5: \quad \dot{z} = \dot{y} - \frac{|\dot{y}|}{g(\dot{y})} z \tag{12}$$

$$c_6: \quad g(\dot{y}) = \frac{F_c}{\sigma_0} + \frac{F_s - F_c}{\sigma_0} e^{-|\dot{y}|/v_s} \tag{13}$$

$$d_4: \quad \dot{z} = \frac{dz}{dt} \tag{14}$$

Here, $F_{fric}$ is friction force, $z$ is an internal state variable, and material dependent parameters are $F_c$, the Coulomb friction, $F_s$, the stiction, $v_s$, the Stribeck velocity, $\sigma_0$ and $\sigma_1$, stiffness and damping coefficients, and $\sigma_2$, a viscous friction coefficient.

Parameters and variables in this model are listed in Tables I and II, respectively.

TABLE I

VALUES OF THE SYSTEM PARAMETERS IN HYDRAULIC UNITS

| Parameter | Value | Parameter | Value |
|---|---|---|---|
| $M$ | = 41 kg | | |
| $k$ | = 11400 N/m | $d$ | = 200 Ns/m |
| $A$ | = 946 $mm^2$ | $\beta$ | = 12665 bar |
| $\rho$ | = 900 $kg/m^3$ | $V_t$ | = 782 $cm^3$ |
| $C_d$ | = 0.65 | $w$ | = 7 $mm$ |
| $p$ | = 80 bar | $c_L$ | = 0 $cm^3$/s/bar |
| $\sigma_0$ | = 5880 N/m | $\sigma_1$ | = 108 Ns/m |
| $\sigma_2$ | = 500 Ns/m | $F_c$ | = 270 N |
| $F_s$ | = 500 N | $v_s$ | = 0.05 m/s |

TABLE II

LIST OF SYSTEM VARIABLES IN HYDRAULIC UNITS

| Variables | Unit | Variables | Unit |
|---|---|---|---|
| $y$ | m | $\dot{y}$ | m/s |
| $p_L$ | bar | $x_v$ | mm |
| $Q_L$ | L/min | $r$ | L/min |

## III. RESIDUAL GENERATION

A formal analysis of analytic redundancy relations, which can be used for residual generation, is obtained from the constraints of the system, Eqs.(1 - 14),

$$\mathcal{C} = \{c_1, c_2, c_3, c_4, c_5, c_6, m_1, m_2, a_1, a_2, d_1, d_2, d_3, d_4\} \tag{15}$$

The unknown variables in these constraints are

$$\mathcal{X} = \{Q_L, x_v, F_{fric}, z, \dot{z}, y, \dot{y}, \ddot{y}, p_L, \dot{p_L}, p\} \tag{16}$$

and the known variables are

$$\mathcal{K} = \{y_1, y_2, u_1, u_2\} \tag{17}$$

A standard structural analysis [11] reveals that the maximal number of analytical redundancy relations are $|\mathcal{C}|-|\mathcal{X}|$ where $|\cdot|$ denote the number of elements in the set, also referred to as cardinality. The three resulting residual generators were found to be quite difficult to work with in practice due to the complex nature of the LuGre model of friction. Instead, a simplified, steady state model is considered.

### A. Steady state model

In steady state, when the mass velocity $\dot{y}$ is constant, Eqs.(11, 1-3) become $s_1$ to $s_4$ below,

$$s_1: \quad F_{fric} = g(\dot{y})\text{sign}(\dot{y}) + \sigma_2\dot{y} \tag{18}$$

$$s_2: \quad Q_L = 6000\sqrt{10}\, C_d\, w\, x_v \sqrt{\frac{1}{\rho}(p - \text{sign}(x_v)p_L)} \tag{19}$$

$$s_3: \quad 0 = \frac{A\, p_L}{10} - ky - d\dot{y} - F_{fric} \tag{20}$$

$$s_4: \quad 0 = Q_L\frac{50}{3} - A\dot{y} - c_L p_L \tag{21}$$

$$m_1: \quad y_1 = y + w_{1n} \tag{22}$$

$$m_2: \quad y_2 = p_L + w_{2n} \tag{23}$$

$$a_1: \quad u_1 = x_v \tag{24}$$

$$a_2: \quad u_2 = p \tag{25}$$

$$d_1: \quad \dot{y} = \frac{dy}{dt} \tag{26}$$

In the set of steady state equations, $\mathcal{C} = \{s_1, s_2, s_3, s_4, m_1, m_2, a_1, a_2, d_1\}$, $\mathcal{X} = \{Q_L, x_v, F_{fric}, y, \dot{y}, p_L, p\}$ and $\mathcal{K} = \{y_1, y_2, u_1, u_2\}$. Therefore there are a maximum of two residuals. This gives the possibility to detect and isolate the leakage and friction faults.

Two unmatched constraints, that can be used for residual generation, are Eqs. 20 and 21.

Eq. (21) is sensitive to detect a leakage, but it is sensitive also to possible faults related to $a_1$, $a_2$, $m_1$ and $m_2$. In a similar way Eq.(20) can be used to detect a fault in friction, if the pressure and position measurements are available, but it is sensitive also to sensor faults in $m_1$ and $m_2$. In the rest of the paper only the leakage detection is considered but the fault detection in friction can be designed using the same methods. Fault isolation is not directly obtainable through passive diagnosis, i.e. by just observing the residuals. Instead active fault diagnosis can be employed where perturbation signals on $u_1$ and $u_2$ cause response signatures in $y_1$, $y_2$ and the two residuals, which depend on the type of fault that is present, see [12], [13] and [14] and references herein.

### B. Residual for leakage detection

During operation, when the system is gripping a drilling pipe, velocity is zero, valve opening $x_v$ is positive and the load pressure is high. Eq.(21) gives in this case the following residual $r$:

$$0 = Q_L\frac{50}{3} - c_L p_L \tag{27}$$

$$r = 10^5\sqrt{10}C_d\, w\, x_v\sqrt{\frac{p - y_2}{\rho}} - c_L y_2$$

$$r = 10^5\sqrt{10}C_d\, w\, x_v\sqrt{\frac{p - p_L}{\rho}}\sqrt{1 - \frac{w_{2n}}{p - p_L}} - c_L(p_L + w_{2n}) \tag{28}$$

Considering $\frac{w_n}{p-p_L} << 1$ an Euler approximation gives:

$$r = 10^5\sqrt{10}\, C_d\, w\, x_v\sqrt{\frac{p - p_L}{\rho}} - c_L p_L + w' \tag{29}$$

where

$$w' = -\left(10^5\sqrt{10}\, C_d\, w\, x_v\sqrt{\frac{1}{\rho}}\,\frac{1}{2\sqrt{p - p_L}} + c_L\right) w_{2n} \tag{30}$$

From Eq.(30) it follows that the noise $w'$ in the residual is also white with gaussian distribution. This assumption will held in the following sections when designing the fault detectors.

The goal of the leakage detector is to decide between two hypothesis. The null hypothesis ($\mathcal{H}_0$), when only noise $w'$ is present in the residual, characterises an acceptable leakage, whereas the alternative hypothesis ($\mathcal{H}_1$), when a constant signal and noise is present in the residual characterises a too high leakage. The probability of false alarm ($P_{FA}$) is chosen by the designer.

## IV. DETECTOR DESIGN FOR UNKNOWN PARAMETERS

### A. Unknown DC levels and noise parameters

In a first step, the time $n_0$ when the fault occurs is supposed to be known. This assumption will be relaxed in a second step. Since the leakage in the cylinder as well as the valve parameters $C_d$, $w$ and $\rho$ are uncertain, the DC level of residual (29) before and after the jump time, respectively $A_1$ and $A_2$ are unknown. The variance of the WGN in the residual depends on the leakage in the cylinder as shown in Eq.(30). It is hence considered as another unknown parameter. The hypothesis testing problem is

$$\mathcal{H}_0 : A_1 = A_2$$
$$\mathcal{H}_1 : A_1 \neq A_2$$

Since this is a composite hypothesis test, the usual general generalised likelihood ration test (GLRT) is applied, which for a signal with unknown parameter vector $\theta$ in WGN, is to decide $\mathcal{H}_1$ if the log-likelihood $L(x)$ exceeds a threshold $\gamma$,

$$L(x) = \frac{p(x; \hat{\theta}, \mathcal{H}_1)}{p(x; \mathcal{H}_0)} > \gamma \tag{31}$$

where $\gamma$ is determined by the desired false alarm probability $P_{FA}$ and $\hat{\theta}$ is the maximum likelihood estimator (MLE) of $\theta$ (maximises $p(x;\theta,\mathcal{H}_1)$).

The probabilities for false-alarm $P_{FA}$and detection $P_D$ are

$$P_{FA} = \int_{\{x:L(x)>\gamma\}} p(x;\mathcal{H}_o)dx \quad (32)$$

$$P_D = \int_{\{x:L(x)<\gamma\}} p(x;\mathcal{H}_1)dx. \quad (33)$$

The MLEs of the DC levels and the variances of the residual before and after the jump time under $\mathcal{H}_0$ (i.e. $\hat{A}$ and $\hat{\sigma_0^2}$) and under $\mathcal{H}_1$ (i.e. $\hat{A}_1$, $\hat{A}_2$, $\hat{\sigma_1^2}$ and $\hat{\sigma_2^2}$ respectively) are determined as follows [4], [5]:

$$\begin{aligned}
\hat{A} &= \frac{1}{N}\sum_{n=0}^{N-1} x[n] = \bar{x} \\
\hat{A}_1 &= \frac{1}{n_0}\sum_{n=0}^{n_0-1} x[n] \\
\hat{A}_2 &= \frac{1}{N-n_0}\sum_{n=n_0}^{N-1} x[n] \\
\hat{\sigma_0^2} &= \frac{1}{N}\sum_{n=0}^{N-1}(x[n]-\hat{A})^2 \\
\hat{\sigma_1^2} &= \frac{1}{n_0}\sum_{n=0}^{n_0-1}(x[n]-\hat{A}_1)^2 \\
\hat{\sigma_2^2} &= \frac{1}{N-n_0}\sum_{n=n_0}^{N-1}(x[n]-\hat{A}_2)^2
\end{aligned} \quad (34)$$

The GLRT decides $\mathcal{H}_1$ if

$$L_G(x) = \frac{p(x;\hat{A}_1,\hat{A}_2,\hat{\sigma_1^2},\hat{\sigma_2^2})}{p(x;\hat{A},\hat{A},\hat{\sigma_0^2},\hat{\sigma_0^2})} > \gamma \quad (35)$$

Assuming Gaussian distributions, which will be verified experimentally in Section V,

$$\frac{p(x;\hat{A}_1,\hat{A}_2,\hat{\sigma_1^2},\hat{\sigma_2^2})}{p(x;\hat{A},\hat{\sigma_0^2})} =$$

$$\prod_{n=0}^{n_0-1}\sqrt{\frac{\hat{\sigma_0^2}}{\hat{\sigma_1^2}}}\exp\left[\frac{1}{2}\left(\frac{(x[n]-\bar{x})^2}{\sigma_0^2}-\frac{(x[n]-A_1)^2}{\sigma_1^2}\right)\right]\times$$

$$\prod_{n=n_0}^{N-1}\sqrt{\frac{\hat{\sigma_0^2}}{\hat{\sigma_2^2}}}\exp\left[\frac{1}{2}\left(\frac{(x[n]-\bar{x})^2}{\sigma_0^2}-\frac{(x[n]-A_2)^2}{\sigma_2^2}\right)\right],$$

hence,

$$2\ln L_G =$$

$$\sum_{n=0}^{n_0-1}\left[\ln\left(\frac{\hat{\sigma_0^2}}{\hat{\sigma_1^2}}\right)+\frac{(x[n]-\bar{x})^2}{\hat{\sigma_0^2}}-\frac{(x[n]-\hat{A}_1)^2}{\hat{\sigma_1^2}}\right]$$

$$+\sum_{n=n_0}^{N-1}\left[\ln\left(\frac{\hat{\sigma_0^2}}{\hat{\sigma_2^2}}\right)+\frac{(x[n]-\bar{x})^2}{\hat{\sigma_0^2}}-\frac{(x[n]-\hat{A}_2)^2}{\hat{\sigma_2^2}}\right]$$

and by using the estimates in Eq. 34,

$$2\ln L_G = N\ln(\hat{\sigma_0^2}) - n_0\ln(\hat{\sigma_1^2}) - (N-n_0)\ln(\hat{\sigma_2^2})$$

Since the logarithm is a monotonic function, the GLRT decides $\mathcal{H}_1$ if :

$$2\ln L_G(x) = N\ln\left(\frac{\hat{\sigma_0^2}}{(\hat{\sigma_1^2})^{\frac{n_0}{N}}(\hat{\sigma_2^2})^{\frac{N-n_0}{N}}}\right) > \gamma' \quad (36)$$

where $\gamma' = 2\ln\gamma$.

### *B. Unknown DC levels and noise parameters and jump time*

To accommodate with unknown jump time, the transition, if it occurs, is assumed not too close to the endpoints of the observation interval. $n_{0_{min}} \leq n_0 \leq n_{0_{max}}$, where presumably $n_{0_{min}} \gg 1$ and $n_{0_{max}} \ll N-1$

$$L_G(x) = \frac{p(x;\hat{n}_0,\hat{A}_1,\hat{A}_2,\hat{\sigma_1^2},\hat{\sigma_2^2})}{p(x;\hat{A},\hat{\sigma_0^2})} > \gamma \quad (37)$$

where $\hat{n_0}$ is the MLE under $\mathcal{H}_1$. Or equivalently,

$$L_G(x) = \frac{\max_{n_0} p(x;n_0,\mathcal{H}_1)}{p(x;\mathcal{H}_0)} \quad (38)$$

Since the PDF under $\mathcal{H}_0$ does not depend on $n_0$ and is nonnegative, the test is also:

$$\max_{n_0}\left(2\ln\frac{p(x;n_0,\mathcal{H}_1)}{p(x;\mathcal{H}_0)}\right) > 2\ln\gamma \quad (39)$$

The GLRT decides $\mathcal{H}_1$ if

$$\max_{n_0}\left(N\ln\left(\frac{\hat{\sigma_0^2}}{(\hat{\sigma_1^2})^{\frac{n_0}{N}}(\hat{\sigma_2^2})^{\frac{N-n_0}{N}}}\right)\right) > \gamma' \quad (40)$$

where, again $\gamma' = 2\ln\gamma$.

### *C. Adaptive threshold*

In order to reduce the time to detect the leakage, to reduce the false alarm rate and to revert to non-faulty case when a fault disappears, a recursive cumulative GLRT with adaptive threshold and upper bounded is implemented. Following is the algorithm for an upper bound $h = 90$ and an initial threshold $\gamma_0 = 30$.

*a) Initialisation:*

$$\begin{aligned} h &= 90 \\ \gamma_0 &= 30 \end{aligned}$$

*b) Loop:*

$$\begin{aligned} g_k &= x_k - \gamma_{k-1} \\ \gamma_k &= x_k - \text{sign}(g_k)\min(|g_k|,\Delta) \\ g_k &= \max(0, g_{k-1}+g_k) \\ g_k &= \min(h, g_k) \end{aligned} \quad (41)$$

*c) Result:*

$$g_k \quad \text{for increasing time } t_k$$

where $x_k$ is the value at time $t_k$ of the statistical test in Eq. (40) and $\Delta$ is the maximum difference between the threshold and the statistical test. The motivation behind the threshold adaptivity is to decrease the time to detect fault reversion.

## V. EXPERIMENTAL MODEL VALIDATION

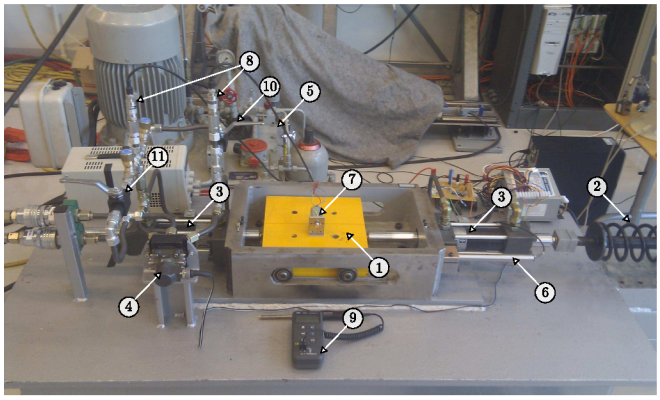


Fig. 2. Test bench. 1: Mass, 2: Mechanical spring/damper, 3: Hydraulic cylinder, 4:Servo-valve, 5:Pressure source, 6: Position sensor (LVDT), 7: Velocity sensor (tachometer), 8: Pressure sensors, 9: Thermometer, 10: Internal leakage flow valve, 11: External leakage flow valve

In order to apply the theory by [5], developed in the previous section for a NHMS, the residual used to detect a fault in leakage needs to be white or uncorrelated. In order to validate this assumption used in the detector degign, an experiment is conducted on the NHMS shown in Fig. 2 whose model and governing equations were presented in section II. Position and velocity of the mass as well as pressure in each of the cylinder chambers are recorded every millisecond by the sensors when the NHMS is in steady state with constant valve opening and during a total time of 100s. [1] Time record of the residual is given in Fig. 3 together with its probability density function (PDF). It results from the analysis of this signal that the distribution can be considered as gaussian. Fig. 4 shows the power spectral density (PSD) of the residual build from experiment data and hereby validates the assumption that the residual is white, i.e. its PSD is flat with frequency up to 900 Hz. Fig. 5, the autocorrelation function plot, also validates the white residual assumption by showing that each sample is uncorrelated with all the others.

From the experiment data, noise present in the load pressure measurement is found to be WGN with standard deviation $\sigma = 0.0963$. The same noise properties will be used in the next section to detect a simulated fault.

[1]This configuration represents the phase when the tool is engaged and the applied force is constant.

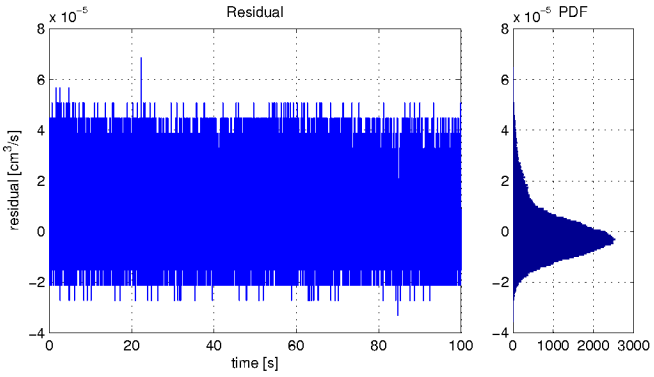


Fig. 3. Residual signal from experiment

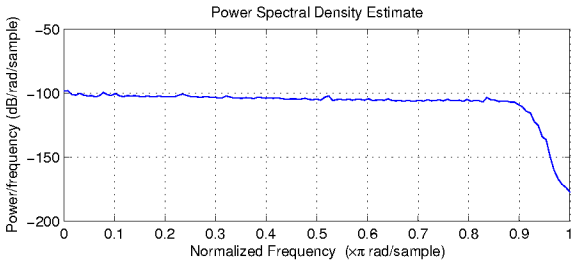


Fig. 4. Power Spectral Density of residual from experiment.

## VI. DETECTION AND PROGNOSIS OF FAULTS

Adjusting with sufficient precision a leakage flow with a correct magnitude to represent a realistic behaviour of a leakage across hydraulic cylinder chambers is a difficult task to realise in practice. First the fault is simulated using the model described in section II. After estimation of the parameters in table I and noise characteristics in section V, the model fits closely to the experimental test bench. A fault occurring between time $t = 14s$ and $t = 15s$ is introduced and is caused by an increase of $0.1cm^3/bar/s$ in the leakage parameter $c_L$. The residual is given in Fig. 6, for a 20 second simulation of the NHMS in steady state with a constant valve opening.

Fig. 7 shows the GLRT values for different jump times. The simulation is run 14.3 s, the real jump time is at 14 s and the GLRT values are given for assumed jump times ranging from 13.1 s to 14.3 s. As expected, the highest value of the GLRT occurs at time close to $t = 14s$ and gives $GLRT = 71.53$, represented by a red dot on Fig. 7.

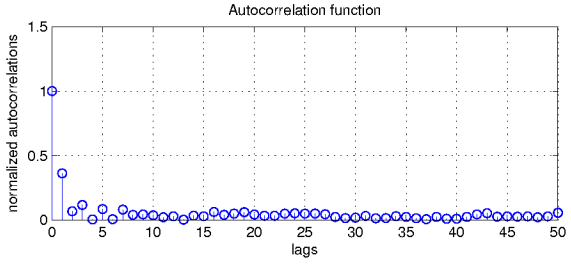


Fig. 5. Normalized autocorrelation function of residual from experiment.

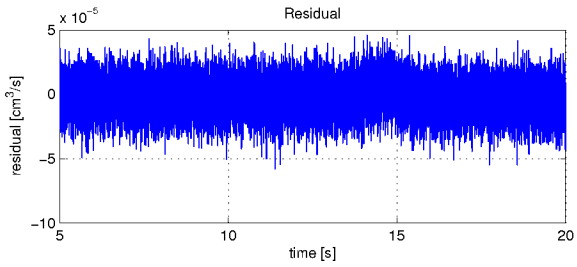


Fig. 6. Residual signal from simulation. Fault in leakage occurs between time $t = 14s$ and $t = 15s$.

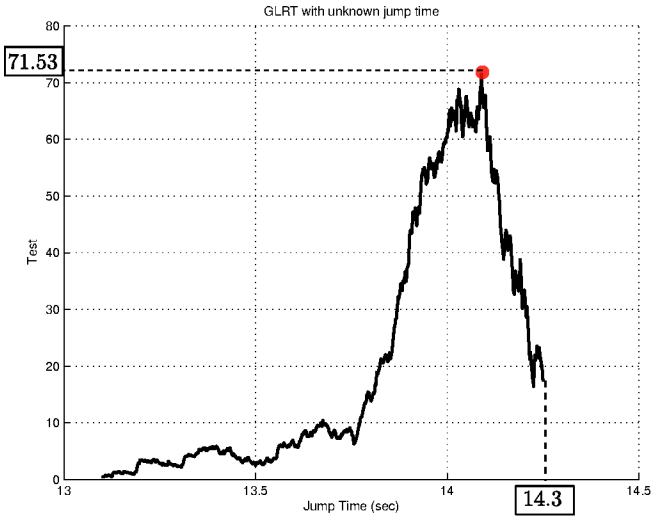


Fig. 7. GLRT for different values of assumed jump time after 14.3s of simulation. (Real jump time = 14s.)

Fig. 8 shows the GLRT with unknown jump time for different simulation end times. For each of these simulation end times a GLRT is run as in the previous figure and the maximum value is returned. The red dot in Fig. 8 hence corresponds to the red dot in Fig. 7. Fault detection is now possible using this last test. For example if the threshold $\gamma$ was fixed at 100, no false alarm would occurs and the time to detect the fault would be $0.4s$.

Running the recursive cumulative GLRT with adaptive threshold and choosing $\Delta = 50$ in order to reduce the time to detect fault reversion, the values $g_k$ are given in Fig. 9. The alarm or stopping time is the smallest time instant at which $g_k$ crosses the given threshold $h_1$. For $h_1$ equal to thirty, detection time is equal to 0.2s. The new detector doesn't trigger any false alarm. The delay of reverting to non-faulty case from faulty is reduced if $h$ is decreased. In the present case, $h = 90$ gives a reverting time equal to 0.25s. In order to prevent the detector from switching excessively between the two cases, the falling edge threshold $h_2$ is taken as half the rising edge threshold, $h_1$. The final fault detection is plotted at the bottom of Fig. 9. The fault cases simulated here demonstrate the ability of the diagnostic method using a somewhat academic case of a fault. The next step is to validate the method with physically developments of leaks. For this purpose the test bench shown in Fig. 2 is run and an

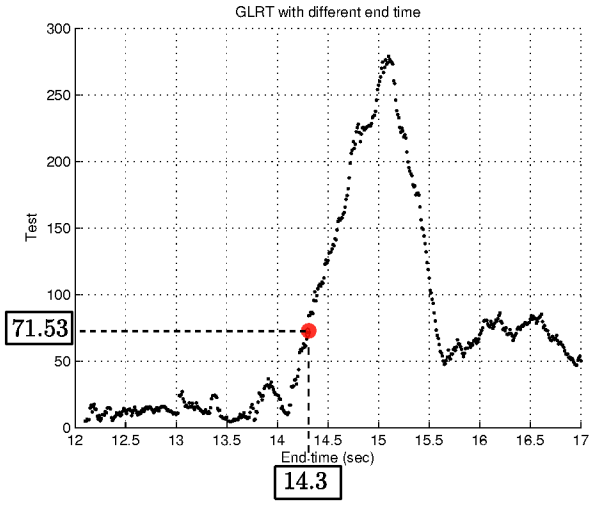


Fig. 8. GLRT with unknown jump time.

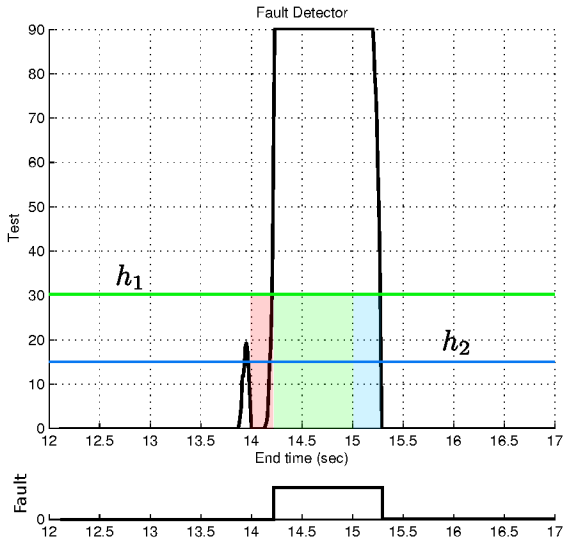


Fig. 9. Fault detector with reversion. Thresholds $h_1 = 30$ (above, a fault is detected) and $h_2 = 15$ (below, a the detected fault is reset) . Real fault occurs between 14 and 15s. Red area is time to detect. Blue area is time to revert to non-faulty case.

internal flow is introduced between the cylinder chambers by opening the valve 10 in Fig. 2, which represent an internal leakage fault. Whereas the mass is maintained constant by the mean of a controller (classical PID controller), the leakage fault is introduced from time $t = 22.5s$ to $t = 5.6s$ with initial non faulty internal leakage equal to 0.9l/min and faulty leakage equal to 1.9l/min, corresponding to an increase of $0.2cm^3/bar/s$ in the leakage parameter $c_L$, i.e. twice as large as the previously simulated fault. The generated residual is shown in Fig. 10. Applying the fault detector designed in section IV, the fault is successfully detected after 0.16s and the time of reverting to non-faulty case is 0.2s (see Fig. 11)

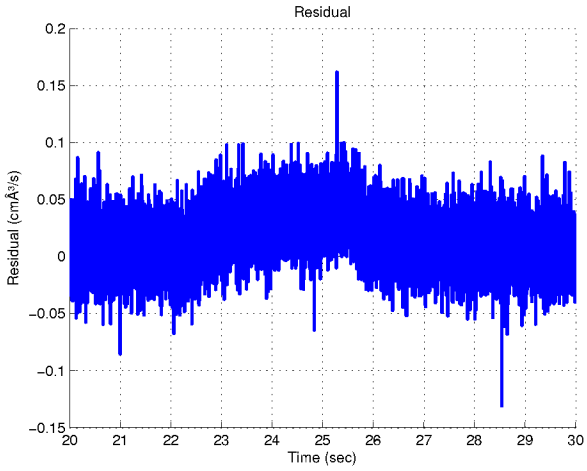


Fig. 10. Residual signal from experiment. Fault in internal leakage occurs between time $t = 22.5s$ and $t = 25.6s$, from 0.9l/min to 1.9l/min. Position of the mass is stabilised around a constant value with a PID controller.

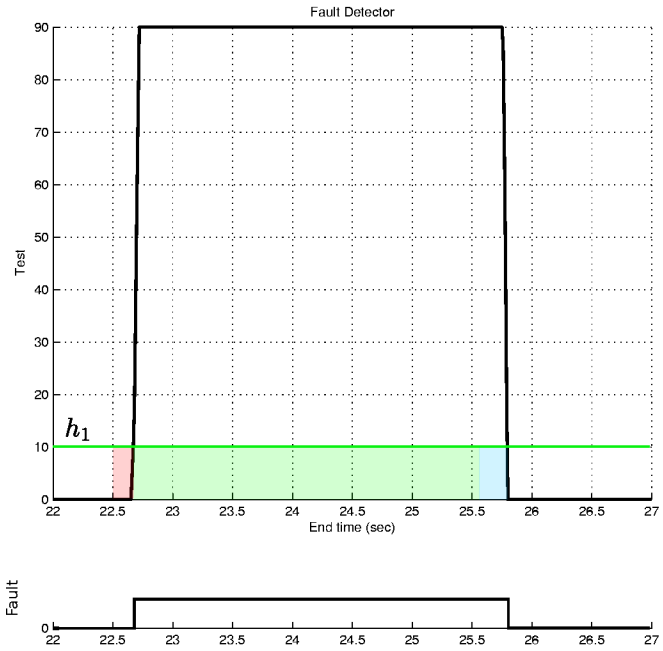


Fig. 11. Fault detector with reversion. Thresholds $h_1 = 10$ (above, a fault is detected). Real fault occurs between 22.5 and 25.6s. Red area is time to detect. Blue area is time to revert to non-faulty case.

## VII. CONCLUSIONS

A fault detector for leakage and increased friction in hydraulic cylinders was developed by initially considering a high fidelity model of a nonlinear hydraulic-mechanical system. Using structural analysis, a robust residual was generated that accommodated unknown parameters and a composite hypothesis test was derived. Test rig measurements were used to validate the properties of residuals and simulation as well as experimental results demonstrated the performance and feasibility of the proposed method regarding prognosis of leakage.

Future research directions are expected to include generalisation of this fault detector to the case of coloured noise in measurements, on real-time implementation on the test rig and on the industrial counterparts in the offshore industry.

## REFERENCES

[1] M. Muenschhof, "Semiphysical Models of a Hydraulic Servo Axis for Fault Detection," *2007 American Control Conference*, pp. 1834–1839, 2007.

[2] L. An and N. Sepehri, "Hydraulic actuator circuit fault detection using extended Kalman filter," *Proceedings of 2003 American Control Conference*, vol. 5, pp. 4261–4266, 2003.

[3] T.-t. Ming, Y.-x. Zhang, and X.-y. Zhang, "Fault detection for electro-hydraulic valve-controlled single rod cylinder servo system using linear robust observer," *2009 International Conference on Measuring Technology and Mechatronics Automation (ICMTMA)*, vol. 1, pp. 639–642, 2009.

[4] M. Basseville and I. V. Nikiforov, *Detection of Abrupt Changes: Theory and Application*, ser. Information and System Science. New York: Prentice Hall, 1993.

[5] S. M. Kay, *Fundamentals of Statistical Signal Processing - Detection Theory*. Prentice Hall PTR, 1998.

[6] F. Gustafsson, *Adaptive Filtering and Change Detection*. Wiley, New York, 2000.

[7] L. Chen and S. Liu, "Fault diagnosis integrated fault-tolerant control for a nonlinear electro-hydraulic system," in *Proc. 2010 IEEE International Conference on Control Applications*, Yokohama, Japan, Sept. 2010.

[8] M. Choux, H. R. Karimi, G. Hovland, M. R. Hansen, M. Ottestad, and M. Blanke, "Robust adaptive backstepping control design for a Nonlinear Hydraulic-Mechanical System," *Proceedings of the 48h IEEE Conference on Decision and Control (CDC) held jointly with 2009 28th Chinese Control Conference*, pp. 2460–2467, Dec. 2009.

[9] M. Choux and G. Hovland, "Adaptive backstepping control of non-linear hydraulic-mechanical system including valve dynamics," *Modeling, Identification and Control*, vol. 31, no. 1, pp. 35–44, 2010.

[10] C. Canudas de Wit, H. Olsson, K. J. Åström, and P. Lischinsky, "A new model for control of systems with friction," *IEEE Trans. on Automatic Control*, vol. 40, no. 3, pp. 419–425, 1995.

[11] M. Blanke, M. Kinnaert, J. Lunze, and M. Staroswiecki, *Diagnosis and Fault-Tolerant Control*, 2nd ed. Springer, 2006.

[12] M. Blanke and M. Staroswiecki, "Structural design of systems with safe behaviour under single and multiple faults," in *Proc. 14th IFAC Safeprocess*, 2006, pp. 474–479.

[13] M. Laursen, M. Blanke, and D. Düstegör, "Fault diagnosis in water for injection system using enhanced structural isolation," *International Journal of Applied Mathematics and Computer Science*, vol. 18 (4), pp. 593–603, 2008.

[14] N. K. Poulsen and H. H. Niemann, "Active fault diagnosis based on stochastic tests," *Internation Journal of Applied Mathematics and Computer Science*, vol. 18 (4), pp. 487–496, 2008.